







RESEARCH ARTICLE



Efficacy of artemether against toxocariasis in mice: parasitological and immunopathological changes in brain, liver, and lung

Dina I. Elgendy ^a, Rasha A. Elmahy ^b, Alaa Ibrahim Mohamed Amer ^c, Hoda A. Ibrahim ^d,
Asmaa Fawzy Eltantawy^e, Fotouh Rashed Mansour ^f and Amina M. Salama ^a

^aMedical Parasitology Department, Faculty of Medicine, Tanta University, Tanta, Egypt; ^bZoology Department, Faculty of Science, Tanta University, Tanta, Egypt; ^cPathology Department, Faculty of Medicine, Tanta University, Tanta, Egypt; ^dMedical Biochemistry Department, Faculty of Medicine, Tanta University, Tanta, Egypt; ^eMedical Pharmacology Department, Faculty of Medicine, Tanta University, Tanta, Egypt; ^fPharmaceutical Analytical Chemistry Department, Faculty of Pharmacy, Tanta University, Tanta, Egypt

ABSTRACT

Toxocariasis is a zoonosis that represents a serious threat to public health particularly in tropical and subtropical areas. Currently, albendazole, the most effective drug for treating visceral toxocariasis, shows moderate efficacy against the larvae in tissues and has some adverse effects. Artemether is an antiparasitic drug mainly used in the treatment of malaria and showed effectiveness against numerous helminthic infections. Besides, it possesses potent anti-inflammatory, antiapoptotic, antifibrotic, and neuroprotective properties. Thus, the study's aim was to investigate artemether's effects in comparison with albendazole on the therapeutic outcome of experimental toxocariasis. For this aim, 140 laboratory-bred mice were divided into four main groups: uninfected control, treatment control, albendazole-treated, and artemether-treated groups. The treatment regimens were started at the 15th dpi (early treatment), and at the 35th dpi (late treatment). The effectiveness of treatment was determined by brain larval count, histopathological, immunohistochemical, and biochemical examination. Artemether showed more effectiveness than albendazole in reducing brain larval counts, markers of brain injury including NF- κ B, GFAP, and caspase-3, the diameter and number of hepatic granulomas, hepatic oxidative stress, hepatic IL-6, and TG2 mRNA, and pulmonary inflammation and fibrosis. The efficacy of artemether was the same when administered early or late in the infection. Finally, our findings illustrated that artemether might be a promising therapy for *T. canis* infection and it could be a good substitution for albendazole in toxocariasis treatment.

KEYWORDS

Toxocara canis; artemether; GFAP; caspase-3; oxidative stress; neuroinflammation; qRT-PCR

Introduction

Toxocariasis is a zoonosis chiefly caused by *Toxocara canis*, which is a frequently occurring intestinal nematode of dogs [1]. It may affect large-scale paratenic hosts including humans. The disease represents a serious threat to public health, particularly in tropical and subtropical areas where its prevalence rate may reach 40% [2]. Human toxocariasis seroprevalence in Egypt was estimated to range from 4.2% to 18.5% [3–5]. Multiple factors involving inflammation, apoptosis, and oxidative stress play a significant role in the pathogenesis of toxocariasis [6–8].

Human toxocariasis includes three distinct clinical syndromes: visceral larva migrans, ocular larva migrans, and covert toxocariasis. The severity of the disease is dependent on the parasite load, the duration of larval migration, age, and patient's immune-mediated reactions [9,10]. The manifestations differ extensively from asymptomatic cases to severe health problems presenting with fever, eosinophilia, gastrointestinal manifestations, hepatosplenomegaly, central nervous system affection, and pulmonary manifestations [11,12].

In the CNS, larval migration and persistence can cause serious CNS insults such as eosinophilic meningitis, encephalitis, myelitis, cerebral vasculitis, or behavioral problems [13–16]. Additionally, there is growing evidence in the literature that neurotoxocariasis may be linked to several neurodegenerative conditions, such as idiopathic Parkinson's disease, Alzheimer's disease, and depression [15,17].

The management of human toxocariasis is challenging because of the limited number of available drugs for its treatment including albendazole, tinidazole, thiabendazole, and diethylcarbamazine [18]. These drugs show moderate efficacy against the larvae in tissues. Unfortunately, anthelmintics used for the treatment of intestinal helminthiasis are generally less effective against tissue parasites including visceral toxocariasis [19]. Albendazole, the preferred medication for treating visceral toxocariasis, has low water solubility, resulting in a low and/or variable bioavailability following its oral administration [20–22]. Besides, it should be administered with fatty meals [23]. It showed moderate efficacy against *T. canis* infection in

mice with therapeutic efficacy rates (45–70%) [24,25]. Moreover, in the treatment of human toxocariasis, it has limited efficacy [26,27]. Additionally, it can cause headache, nausea, dizziness, constipation, alopecia, occasionally abnormal liver function tests, and acute and granulomatous hepatitis [28–32]. Consequently, it is important to find safer and more effective alternatives for the treatment of this serious infection.

Artemether is a lipid-soluble derivative of artemisinin [33], abundant in the remedy plant *Artemisia annua* [34]. It is a well-tolerated antimalarial drug with no significant adverse effects on humans [35–37]. It also showed effectiveness against *Schistosoma* species both in vitro and in vivo [38]. Moreover, artemisinin and its derivatives have antiparasitic effects on other parasites such as *Leishmania* spp., *Acanthamoeba* spp., and *Taenia* spp. [39, 40]. Besides, it possesses potent anti-inflammatory, antifibrotic, immunomodulatory, and neuroprotective effects [41–44]. Recently, the action of artemisinin on some roundworms began to attract attention [45]. It was tested in vitro on the adult of *T. canis*, the results were found promising [39]. However, artemether was never investigated in the treatment of toxocariasis in experimental animals. Curiously, artemether could be a promising candidate for drug repurposing against toxocariasis. Therefore, this work aims to explore the therapeutic effects of artemether in experimental toxocariasis, in comparison with albendazole.

Material and methods

Type of the study

An experimental study was conducted in the Medical Parasitology, Pathology, and Biochemistry Departments, Faculty of Medicine, Tanta University, and the Zoology Department, Faculty of Science, Tanta University.

Ethical considerations

The authors affirm that all methods used in this study adhered to the ethical guidelines of the relevant national and institutional guides on the care and use of laboratory animals. This research work was approved by the Laboratory Animal Centre for Research Ethics Committee, Faculty of Medicine, Tanta University (Approval code number 36,087/11/22).

Drugs

Albendazole: (Alzental; suspension of 100 mg/5 ml, Eipico Pharm Co., Egypt). It is soluble in water. After appropriate dilution with sterile distilled water, a dose of 100 mg/kg was given to each mouse once daily for 5

consecutive days [46]. Artemether: (Hepalin; 100 mg tablet, Well care pharmaceutical company, U.S.A.) was dissolved, just before treatment, in a mixture of 3% ethanol, 7% Tween 80, and diluted with distilled water. It was administered to each mouse in two doses of 400 mg/kg each and two weeks apart [45]. The required dose of each drug was adjusted to be in a volume not exceeding 0.25 ml. The fine suspension of each drug was administered by oral gavages to each mouse.

Experimental animals

Seventy male Swiss albino mice, 6–8 weeks old, weighing 20–25 g were obtained from Theodore Bilharz Research Institute (Giza, Egypt). They were kept in accordance with institutional and national guidelines. These mice were used in the experiment after a 7-day acclimatization period.

Toxocara canis infection

T. canis eggs were retrieved from the uteri of gravid females collected from naturally infected puppies. After that, the eggs were cultivated in 0.1N H₂SO₄ for embryonation and storage. Infection was performed utilizing eggs from cultures that were no older than 8 weeks [47]. The eggs were rinsed three times in physiological saline to remove the physiological saline/H₂SO₄ solution before the mice were infected. The eggs were suspended in distilled water with a concentration of 1000 viable embryonated eggs per 0.25 ml. Each mouse in the infected groups was infected with 1000 embryonated eggs by intragastric injection [48].

Experimental design

Mice were divided into four groups:

Group I (uninfected control) (10 mice): served as the uninfected untreated control.

Group II (treatment control) (20 mice): *T. canis*-infected untreated mice. They were split into two equal subgroups; IIa (early treatment control). The mice of this group were sacrificed on the 30th dpi, and IIb (late treatment control). The mice of this group were sacrificed on the 50th dpi.

Group III (albendazole treated) (20 mice): *T. canis*-infected mice that received albendazole treatment. This group was split into two subgroups (10 mice each); group IIIa was treated with albendazole starting on the 15th dpi. (early albendazole), and group IIIb was treated with albendazole starting on the 35th dpi (late albendazole).

Group IV (artemether treated) (20 mice): *T. canis*-infected mice that received artemether treatment. This group was also split into two subgroups (10 mice each); group IVa was treated with artemether

starting on the 15th dpi (early artemether), and group IVb was treated with artemether starting on the 35th dpi (late artemether).

On the 30th dpi, 5 mice from each of the groups (I, IIa, IIIa, and IVa) were sacrificed. Their brains, livers, and lungs were taken and a similar piece from each sample was used for histopathological study, immunohistochemical study, and biochemical analysis. The brain was divided longitudinally into two halves the left side of the brain was used for histopathological and immunohistochemical studies. The right side of the brain was used for biochemical analysis by ELISA. Another five mice from each of the groups (IIa, IIIa, and IVa) were sacrificed and their whole brains were used for brain larval counting. On the 50th dpi, the same steps were done with the remaining groups.

Parasitological study

Total brain larval counts

After the infected mice were sacrificed, the entire brain of each mouse was removed in a clean Petri dish. The cerebrum and the cerebellum's two halves were split, and each half was squeezed between two microscopic slides before being examined under a light microscope (low power). The larvae were counted immediately by direct microscopic counting. Their motility was observed in each half then we added the numbers of larvae detected in both halves together to calculate the total number of larvae per brain [47].

Histopathological and immunohistochemical assessment

Hematoxylin and eosin staining

Tissue samples obtained from the brains, livers, and lungs of the studied groups were in the form of formalin-fixed paraffin-embedded tissue blocks. Blocks were cut into sections by microtome and then stained with (H&E). The slides were examined for histopathological changes in the treatment control group in comparison with the treated groups. For brain specimens, the detection of larvae in the parenchymal tissue of the brain sections from the infected and treated animals was done and the inflammatory reaction was assessed. For liver specimens, remains of larvae in hepatic parenchyma and granulomatous reaction were determined. For assessment of granuloma number, examination of 5 histological sections per mouse, an inspection of 10 high-power fields (x400) in each section was done and followed by calculation of the average number. Furthermore, the widest diameter of the granulomas was measured using the Image J software (Image J bundled with plugins) (<http://fiji.sc>), and then the mean diameter of the granulomas was calculated.

For lung specimens, histopathological evaluation of the degree of inflammation, cellular infiltration around bronchi, alveoli, or blood vessels, formation of lymphoid follicles, patchy fibrosis, and fibroblastic foci was done. Histopathological changes were graded from 0 to +3. The criteria of grading were 0 for normal lung, +1 for mild inflammation with minimal fibrous thickening, +2 for moderate inflammation with moderate fibrous thickening, and +3 for severe inflammation with marked fibrosis [49]. The examination of all tissue sections and scoring were carried out blindly.

Masson's trichrome staining of lung sections

Masson's trichrome staining was utilized to highlight connective tissue formation. Paraffin-embedded tissue blocks were cut into 4- μ m sections. Staining was done using an automated tissue stain according to staining protocol. Finally, the slides were dehydrated in ascending series of ethyl alcohol, cleared in Xylol and mounted in D.P. X [50].

GFAP and caspase-3 immunohistochemical staining

Paraffin blocks sections of 3 μ m thickness, were mounted on positively charged slides. Antigen retrieval in Dako PT Link unit using high pH EnVision™ FLEX antigen retrieval solutions reaching a temperature of 97 °C for 20 min was performed. Slides were transferred to Dako Autostainer Link 48. The internal peroxidase activity was blocked, followed by incubation with primary antibodies for 30 min with subsequent addition of detection system for 20 min, chromogen (Diaminobenzidine, DAB) for 10 min. At the end of the staining run, slides were flooded with distilled water and counterstained with hematoxylin. Later, an overnight incubation was done with rabbit polyclonal anti-GFAP antibody (Cat. No. Z0334, 1: 100 dilution, Dako, U.S.A.), and rabbit polyclonal anti-caspase-3 (Cat. No ab4051, 1:50 dilution, Abcam, U.S. A.). Negative controls were prepared by replacing the primary antibody with PBS. Finally, slides for visualization were prepared using DPX mount and analyzed using Olympus Bx 50 microscope [51].

Interpretation of GFAP positivity

GFAP staining reaction was predominantly cytoplasmic. The extent of positivity was scored according to the number of the stained cells and the intensity of the staining as follows: negative (0), scattered with weakly positive staining; (+1), a cluster of cells (20%–50%) with moderately positive staining (+2), and (50%–90%) of cells with strongly positive staining (+3) [52].

Interpretation of caspase-3 positivity

Caspase-3 positivity was diagnosed in the cytoplasm by a brownish stain. The score was calculated by multiplying the intensity score by the percentage of stained cells. The caspase-3 intensity was assessed semi-quantitatively as the following: negative (0), weak staining (+1), moderate staining (+2), or strong staining (+3). The stained cell percentages were determined as follows: 0 (<5% of cells); +1 (5–20% of cells); +2 (21–50% of cells), and +3 (>50% of cells). The final scoring was: Negative (0 points), +1 (1–3 points), +2 (4, 6 points), and +3 (9 points) [53].

Biochemical assessment

Preparation of tissue homogenates

Brain and liver tissue samples from the study groups were removed, cleaned with ice-cold saline, sliced into numerous tiny pieces, weighed, and then homogenized with 50 mM phosphate buffer (pH 7.4). After centrifuging the mixture at 12,000 g for 20 min at 4°C, the insoluble materials were removed from the mixture, and the clear supernatant was then frozen at –80°C for use in biochemical tests.

Oxidative stress assessment in liver tissue homogenates

Malondialdehyde (MDA) (CAT# MD 25 29), superoxide dismutase (SOD) (CAT# SD 25 21), and catalase (CAT# CA 25 17) commercial kits were used to spectrophotometrically measure the levels of MDA (a biomarker to assess the level of oxidative stress), SOD (a powerful antioxidants defense in almost all living cells), and catalase (an important enzyme in defending the cell against oxidative damage).

Assay of IL-6 in liver tissue homogenates and NF-κB in brain tissue homogenates by ELISA

IL-6 level in liver homogenate was measured using an ELISA kit provided by Abcam company, U.S.A. (CAT# ab222503). Brain homogenate NF-κB was evaluated using commercially available ELISA kits from the Abcam company, U.S.A. (CAT# ab176648). All ELISA techniques were read using a microplate ELISA reader (Stat Fax®2100, Fisher Bioblock Scientific, France) at 450 nm with a correction wavelength set at 570 nm in accordance with the manufacturer's guidelines.

qRT-PCR analysis of relative TG2 mRNA expression in liver homogenates

Total RNA was isolated from the frozen liver homogenate using a Qiagen RNeasy Total RNA isolation kit (Qiagen, Hilden, Germany), as directed by the manufacturer. In line with the instructions of the manufacturer, PCR reactions were carried out using the Power SYBR Green PCR Master Mix (Life Technologies,

Carlsbad, California, U.S.A.). The amount of TG2 mRNA transcript was quantified using the housekeeping gene GAPDH as an internal control. These sequence-specific primers were made in the manner described below: mice TG2 (Gene Bank accession NM_001323317): up-stream: 5'- CACTTTGAGGGCCGCAACTA-3', down-stream: 5'- GTACACAGCATCCGCGGTC-3' with amplicon size 75 bp, mice GAPDH (Gene Bank accession NM_002046.7): up-stream: 5'- CTCTCTGCTCCTCCCTGTTCTA -3' and down-stream: 5'- GCCAAATCCGTTCA CACCGA -3' with amplicon size 112 bp. The thermal cycling conditions were as follows: The first denaturation at 95 °C for 10 minutes was followed by 40 cycles of initial denaturation at 95 °C for 15 seconds, annealing at 60 °C for 30 seconds, and extension at 72 °C for 30 seconds. At the end of the preceding cycle, the temperature was increased from 60 to 95 °C for melting curve analysis. The values of the target and reference genes were used to compute relative gene expression automatically using the comparative threshold (Ct) method and the 2-ΔΔCT formula [54].

Statistical analysis

Data were demonstrated as arithmetic mean ± standard deviation (SD). Analysis of variance (ANOVA) was used to analyze the difference among the means of more than two groups and Post hoc test to determine the probability of significant differences among these groups (for biochemical indices), and Monte Carlo exact test for chi-square (for histopathological and immunohistochemical scores). When ($P < 0.05$), differences were considered significant. Statistical analysis was performed using SPSS 21.0 software (SPSS, Inc., Chicago, IL, U.S.A.). The percentage of reduction was calculated by the equation: Reduction % = $(A - B) / A \times 100$, where A is the mean number of detected larvae from mice of the treatment control group and B is the mean number of detected larvae from treated mice at the same time point post-infection.

Results

Parasitological results

Total brain larval counts

As shown in Table 1, the mean larval counts in the brains of the early albendazole group and early artemether group were significantly lower than that of the early treatment control group ($P = 0.001$) with percentages of reduction 35.5 % and 43.9%, respectively. Similarly, our results revealed a significant reduction in total brain larval counts in the late albendazole group and late artemether group compared to the late treatment control group ($P = 0.001$) with percentages of reduction 33.6% and 37.7%, respectively. Moreover, the groups that received artemether showed significantly lower brain larval counts than

Table 1. Brain larval counts in the infected groups ($n = 5$).

	Early Treatment control (G IIa)	Early Albendazole (G IIIa)	Early Artemether (G IVa)	Late Treatment control (G IIb)	Late Albendazole (G IIIb)	Late Artemether (G IVb)
Larval count in the brain	137.00 ± 7.31	88.40 ± 8.05 ^a	76.80 ± 4.21 ^{a, b}	190.00 ± 6.40 ^{a, b, c}	126.20 ± 3.27 ^{a, b, c, d}	118.40 ± 2.41 ^{a, b, c, d, e}
% Of Reduction		35.5 %	43.9%		33.6%	37.7%
F test				249.543		
P value				0.001*		

* $P < 0.05$ (Significant).

n = number of studied mice in each group.

a: Significant compared with early treatment control, b: Significant compared with early albendazole, c: Significant compared with early artemether, d: Significant compared with late treatment control, & e: Significant compared with late albendazole.

% Of Reduction: % Of Reduction of each group compared to the treatment control group at the same time point post-infection.

the corresponding groups that received albendazole at both time points post-infection. All the larvae found in the brains of the treatment control animals were actively moving through the tissue. They were clustered rather than dispersed randomly throughout the brain tissue. The larvae found in the brains of the treated animals showed reduced motility compared to the treatment control group.

Histopathological findings

Histopathological study of the brain sections stained with H&E

Larvae of *T. canis* were distinguished inside the brain tissue of the treatment control group at both studied times after infection, but there was no cellular inflammatory infiltrate around them (Figure 1 a& b). In comparison to the treatment control group, fewer larvae were found in the brain sections of the treated groups (Figure 1c–f).

Histopathological study of the liver sections stained with H&E

According to the mean number and diameter of granulomas per hepatic section of different studied groups, there was a statistically significant reduction ($P = 0.001$) in the groups that received albendazole and artemether treatment in comparison to the treatment control group. (Figure 2g, h).

Histopathological examination of the liver sections from the early treatment control group (Figure 2a) showed multiple cellular-type granulomas. Furthermore, granulomas from the early albendazole group (Figure 2c), the early artemether group (Figure 2e), and the late artemether group (Figure 2f) were mainly of the cellular type while granulomas from the late treatment control group (Figure 2b), and the late albendazole group (Figure 2d) were mainly of the fibro-cellular type.

Histopathological study of the lung sections stained by H&E and Masson's trichrome

Lung sections from the treatment control group underwent histopathological evaluation, and it was

observed that there was a dense inflammatory cellular infiltrate. Besides, patchy fibrosis and fibroblastic foci were detected (grade +3) (Figure 3a, b). According to the results of the examination of lung sections obtained from all treated groups, an apparent decrease in the intensity of the inflammation was noticed with a reduction in fibrosis in comparison to the treatment control group (Figure 3c–f) (Table 2).

Masson's trichrome staining helped in the detection of collagen deposition in lung sections of all studied groups. Sections from the treatment control group showed a thick deposition of collagen around the alveoli and bronchi (Figure 4a, b). There was a significant decrease in the percentage area of collagen fibers in both albendazole treated and artemether treated groups in comparison with the treatment control group (Figure 4c–g).

Immunohistochemical expression of GFAP and caspase-3 in the brain sections of the studied groups

The immunoreactivity of GFAP (Figure 5) and caspase 3 (Figure 6) in brain tissues were evaluated in all studied groups. The treatment control group showed the highest positivity of the stains (grade +3) compared to the expression in all treated groups. The weakest staining intensity was detected in the groups that received artemether (grade +1) (Figure 5e, f and 6e & 6f). The scores of both markers in different groups are illustrated in Table 3.

Biochemical assessment

Assay of oxidant\antioxidant markers

The late treatment control group showed a greater increment in levels of MDA than the early-treatment control as compared to the uninfected control group. In contrast, early artemether showed a greater decrement in levels of MDA as compared to late artemether and albendazole-treated groups. MDA levels decreased in early albendazole as compared to late albendazole. A significant difference was observed in MDA levels among all groups of the study ($P < 0.001$) as shown in (Figure 7a).

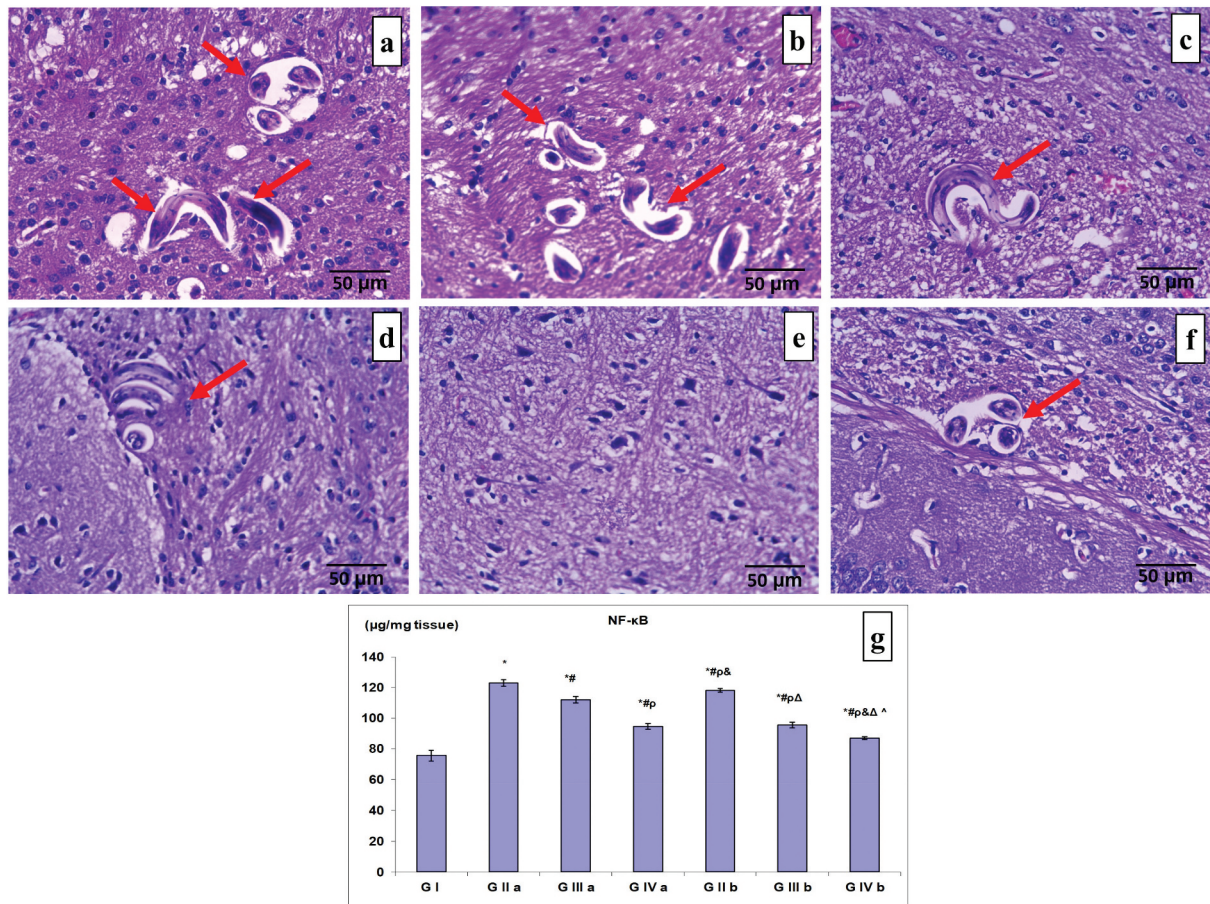


Figure 1. Histopathological findings of brain sections (H&E \times 400, a-f) and the levels of NF- κ B in the brain homogenates (g): (a) early treatment control group showing multiple tangential and transverse sections in *T. canis* larvae (red arrow) without any inflammatory cellular infiltrate surrounding them. (b) late treatment control group showing tangential sections in *T. canis* larvae (red arrow) with no inflammatory reaction. (c) early albendazole group showing a tangential section in *T. canis* larva. (d) late albendazole group showing multiple tangential and transverse sections in *T. canis* larvae (red arrow). (e) early artemether group showing no *T. canis* larvae. (f) late artemether group showing transverse sections in *T. canis* larvae (red arrow). (g) bar chart showing the means of levels of NF- κ B in the brain homogenates in all studied groups. * significant with G I, # significant with G II a, ρ significant with G III a, & significant with G IV a, Δ significant with G II b and ^ significant with G III b.

The early treatment control showed a greater decrement in SOD and catalase levels than the late treatment control as compared to the uninfected control. However, the late artemether showed a greater increment in levels of SOD and catalase as compared to the early artemether group. SOD and catalase levels increased in the late albendazole as compared to early albendazole. Significant differences were observed in SOD levels between all studied groups (Figure 7b). Non-significant differences were observed for catalase levels between early artemether and late albendazole groups as well as between uninfected control and late artemether groups as shown in (Figure 7c).

IL-6 in the liver homogenates and NF- κ B in the brain homogenates

The early treatment control group showed a greater increment in levels of IL-6 and NF- κ B than the late treatment control group as compared to the uninfected control. Nevertheless, as compared to early artemether and albendazole-treated groups, late

artemether showed a greater decrement in levels of IL-6 and NF- κ B. The IL-6 and NF- κ B levels decreased in late albendazole as compared to early albendazole as shown in (Figure 7d) and (Figure 1g) respectively.

Assay of liver homogenate relative TG2 mRNA expression

The relative liver TG2 mRNA expression increased significantly between the infected and uninfected control groups. When compared to the treatment control groups, the treated groups showed statistically significant downregulation in relative liver TG2 mRNA expression ($P < 0.001$). The late artemether group showed the greatest downregulation in liver TG2 mRNA expression when compared to the other treatment groups as demonstrated in Figure 7e.

Discussion

In paratenic hosts including humans and mice, *T. canis* larvae migrate throughout the body for extensive periods [55]. Their migration pathway has been detected in a variety of laboratory animals and mice are the most

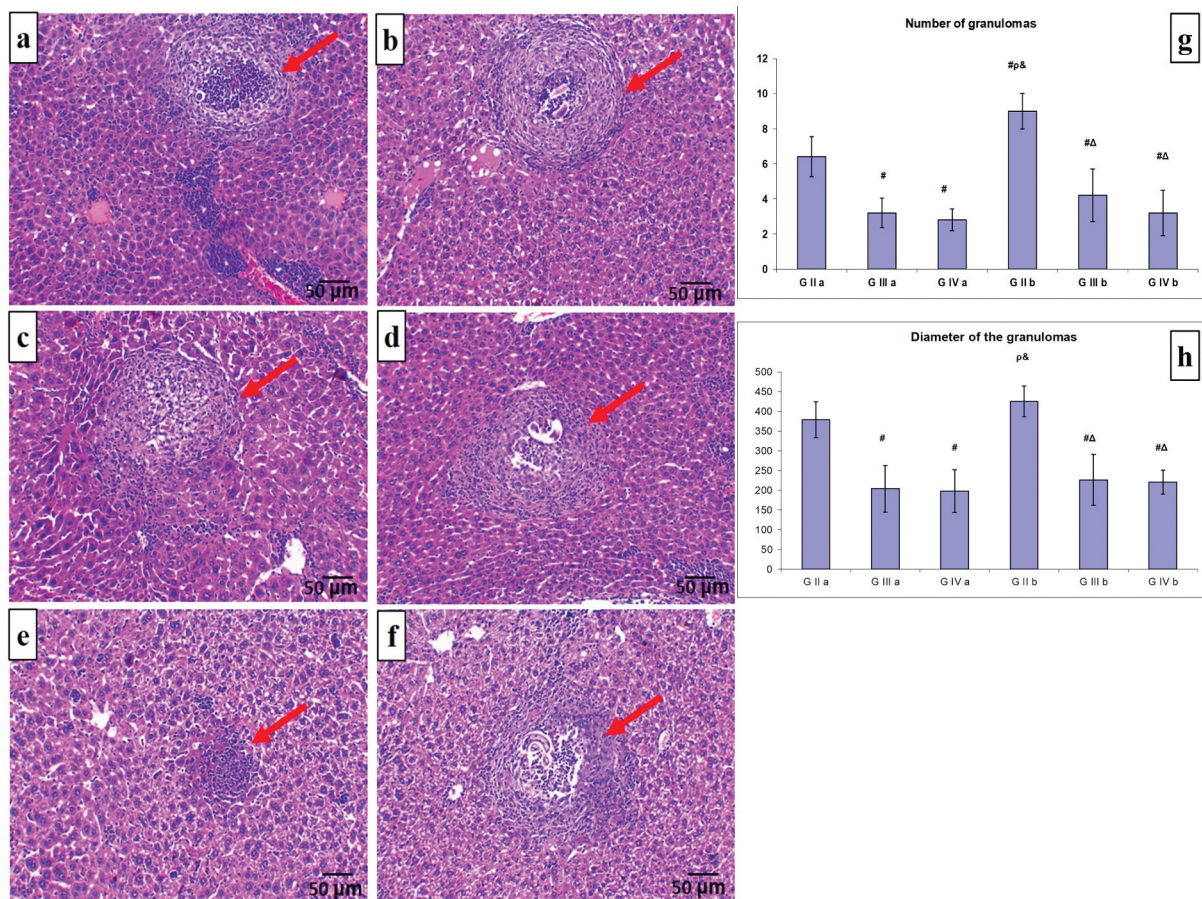


Figure 2. Histopathological findings of liver sections (H&E $\times 200$) (a) early treatment control group showing multiple cellular granulomas consisting of eosinophils, histiocytes, and epithelioid cells (red arrow). (b) late treatment control group showing fibrocellular consisting of fibroblasts and few histiocytes around larvae (c) early albendazole group showing a granuloma of cellular type with scanty fibrous tissue and decrease in granuloma size (red arrow). (d) late albendazole group showing fibrocellular granulomas (red arrow). (e) early artemether group showing reduction of the size of cellular granuloma (red arrow). (f) late artemether group showing cellular granuloma consisting of eosinophils, histiocytes, and epithelioid cells around larvae (red arrow). (g) bar chart showing the means of hepatic granulomas' numbers in infected mice. (h) bar chart showing the means of hepatic granulomas' diameters in infected mice. # significant compared with G II a, p significant compared with G III a, & significant compared with G IV a, Δ significant compared with G II b, and \wedge significant compared with G III b.

dominant animal model [56]. In mice, after piercing the intestinal wall, larvae spread to the liver, lungs, and throughout the body, finally settling in the brain and muscles [57]. In the present work, we investigated the different effects of *T. canis* infection on the livers, lungs, and brains of infected animals and studied the efficacy of artemether in comparison with albendazole in alleviating these effects.

T. canis larvae exhibit a strong neuroaffinity with a preference for the cerebrum [58]. So, the parasite burden in the brain indicates the drug efficacy. In this work, the brain larval counts in the late treatment control group were significantly higher than in the early treatment control group. These observations agree with the findings of [59,60]. Because the brain is believed to be an immune-privileged area where the larvae are sheltered from the immune reaction of the host, the growing accumulation of larvae there may be due to the environment that is most suitable for their survival [61].

Additionally, our findings demonstrated a significantly lower number of brain larvae in treated animals compared to the treatment control animals. Furthermore, in comparison to mice given albendazole, mice that received artemether had significantly lower brain larval counts. This decrease in larval counts could be attributed to the effect of artemether on larval structure, particularly the tegument, or because it inhibits or destroys larval protein activity. These results are consistent with the *in vitro* investigation by [39] who found that artemether had a significantly direct effect on the cuticle of adult *T. canis* than albendazole. It induced lips swallowing with disruption of some sensory papillae. Consequently, these tegumental changes could be considered as an indicator of the probable effects of artemether on *T. canis* larvae. As far as we know, it is the first time to assess the efficacy of artemether against *T. canis* infection *in vivo*. Regarding nematocidal activity of artemether, the preceding study by [45] reported its ability to induce damage to

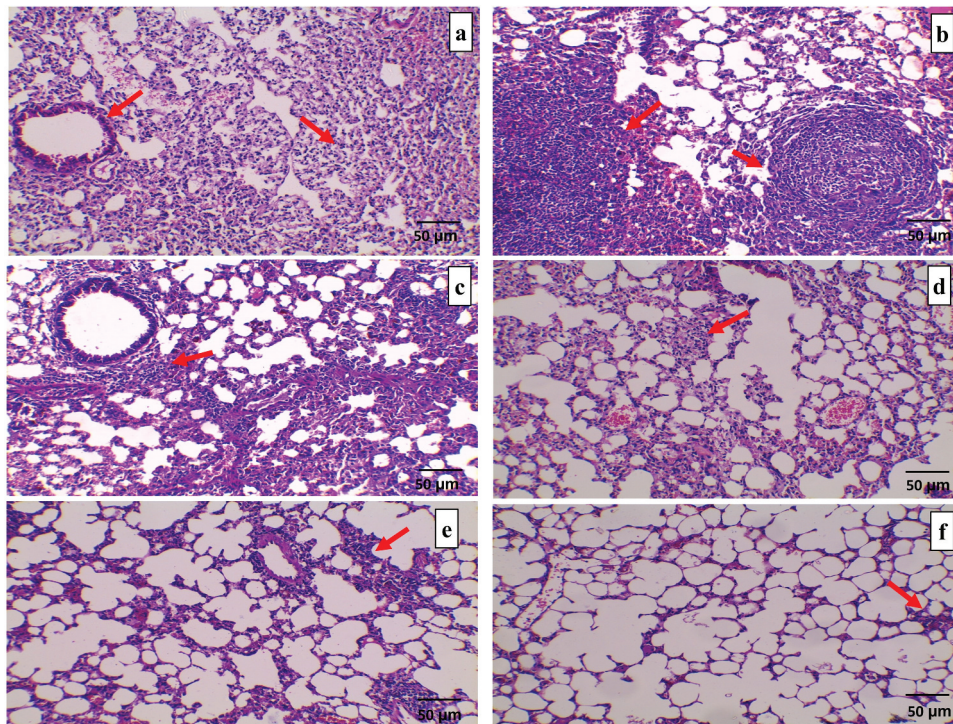


Figure 3. Histopathological findings of lung sections (H&E $\times 200$) (a) early treatment control group showing dense inflammatory cellular infiltrate observed around alveoli (red arrow). (b) late treatment control group showing heavy cellular infiltration around alveoli with granulomatous reaction (red arrow). (c) early albendazole group showing moderate inflammatory infiltrate around alveoli and bronchi. (d) late albendazole group showing a decrease in the inflammatory cellular infiltrate (red arrow). (e) early artemether group showing the reduction in the intensity of the inflammatory cellular infiltrate (red arrow). (f) late artemether group showing more reduction in the intensity of the inflammatory infiltrate (red arrow).

Table 2. Histopathological findings in lung sections of studied groups ($n = 5$).

Groups	Histopathological changes in the lung (score)		
	+1	+2	+3
Early treatment control (G IIa)	0	4	6
Early albendazole (G IIIa)	7	2	1
Early artemether (G IVa)	7	3	0
late treatment control (G IIb)	0	2	8
Late albendazole (G IIIb)	4	4	2
Late artemether (G IVb)	6	4	0
X ²		35.089	
P value		0.001*	

* $P < 0.05$ (Significant).

n = number of studied mice in each group.

Chi-square (X²) test of significance.

the cuticle of adult *Trichinella spiralis* with a significant reduction in adult worm and total larval counts in the tissues of infected mice. In the same context, artemisinin and its derivatives were found to have a powerful antiparasitic effect on adult worms of *Schistosoma mansoni* and *S. japonicum* and their larval stages, causing a reduction in both adult worm and egg counts [62,63]. Furthermore, artemisinin is thought to kill parasites by causing protein destruction and interfering with parasite proteasome activity [64–66].

Histopathological examination of the brain tissues of the infected control group showed the absence of

inflammatory cellular infiltration around the larvae. These results match the findings of preceding studies on *T. canis*-infected outbred mouse strains [60,67,68]. Nevertheless [69], noticed perivascular cuffs comprising of eosinophils and neutrophils in *T. canis*-infected C57Bl/6 mice. This could be attributed to the variation in immunological responses to *T. canis* infection between inbred and outbred mice.

T. canis larvae mechanisms to invade and harm the brain parenchyma have not yet been fully understood [70]. In this context, specific markers may have a role in the migration of larvae as well as the production of degenerative CNS alterations. Therefore, we investigated the alterations in the expression of GFAP, caspase-3, and NF- κ B in the brain of *T. canis*-infected mice. These markers are highly implicated in the pathogenesis of neuroinflammation, neurodegenerative, and traumatic brain injury [71–74].

Astrocytes play a crucial role in the CNS's metabolic processes, neurotransmitter levels regulation, blood-brain barrier maintenance, immunological defense, and other processes that support neuronal homeostasis [75]. Additionally, they have a major role in scar formation, synaptic degeneration and inflammatory mediators secretion. In addition, reactive astrocytes have an essential role in restricting the spread of brain-

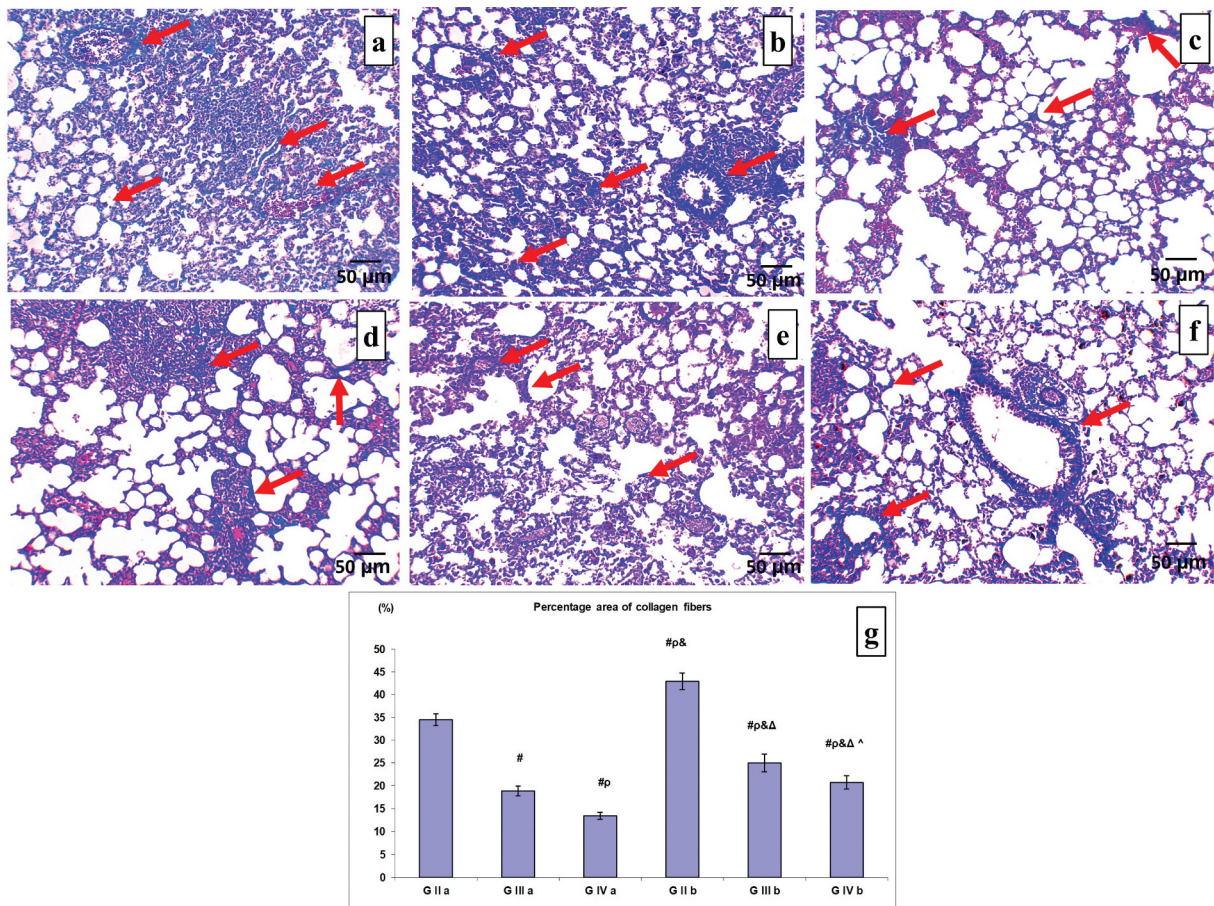


Figure 4. Lung section (Masson's trichrome $\times 200$) (a) early treatment control group showing dense collagen deposition observed around alveoli (red arrows). (b) late treatment control group showing heavy collagen deposition around the alveoli and bronchi (red arrows). (c) early albendazole group showing reduction of collagen formation. (d) late albendazole group showing a decrease in collagen formation (red arrows). (e) early artemether group showing more reduction in collagen deposition (red arrows). (f) late artemether group showing more reduction in collagen deposition (red arrows). (g) bar chart showing the means of percentage areas of collagen fibers in lung sections of studied groups. # significant compared with G II a, p significant compared with G III a, & significant compared with G IV a, Δ significant compared with G II b, and ^ significant compared with G III b.

invading microbes and neurophilic HIV-1 [76,77]. However, they may undergo functional changes upon inflammation or brain injury [78,79].

GFAP is a well-established indicator of astrocyte injury and astrogliosis in different CNS diseases [73]. Astrocytes may respond by rapidly producing extra GFAP in response to blood-brain barrier damage, and excessive GFAP expression states for the maintenance of the blood-brain barrier integrity after being damaged by invading microbial pathogens [80]. Recently, the FDA authorized GFAP as one of the blood-derived brain protein biomarkers in the diagnosis of neurological diseases [81].

In the present work, there was a significant increase in GFAP staining intensity in the brain tissues of treatment control mice with significant upregulation in the late treatment control group compared to the early treatment control group. In line with our findings [67], detected enhanced GFAP mRNA expressions in mice infected with *T. canis* from the 4th to 8th weeks post-infection. Additionally, our results showed significant downregulation in the expression of GFAP in all

treated groups in comparison to the treatment control group. The weakest staining intensity was detected in the groups that received artemether. These results align with [82] who reported that artemether down-regulated the expression of neuroinflammatory marker GFAP in *Plasmodium berghei*-infected mice.

NF- κ B is a main component in almost all kinds of brain cells [83]. Within astrocytes, the activation and enhanced expression of NF- κ B had been stated to significantly augment the degeneration of neurons [84,85]. Our results showed a significant increment in the levels of NF- κ B in the brains of the treatment control mice through the duration of the infection. Similarly [86], reported parallel results in a mouse model of neurotoxocariasis. Likewise [87], denoted that excretory/secretory proteins of adult worms of *T. canis* stimulated the transcriptional and translational levels of NF- κ B expression in mouse macrophages after 9 h of in vitro incubation. In the present work, artemether was superior on albendazole in the reduction of NF- κ B levels in the brain tissues of infected mice. The effects of artemether on the levels of NF- κ B in this

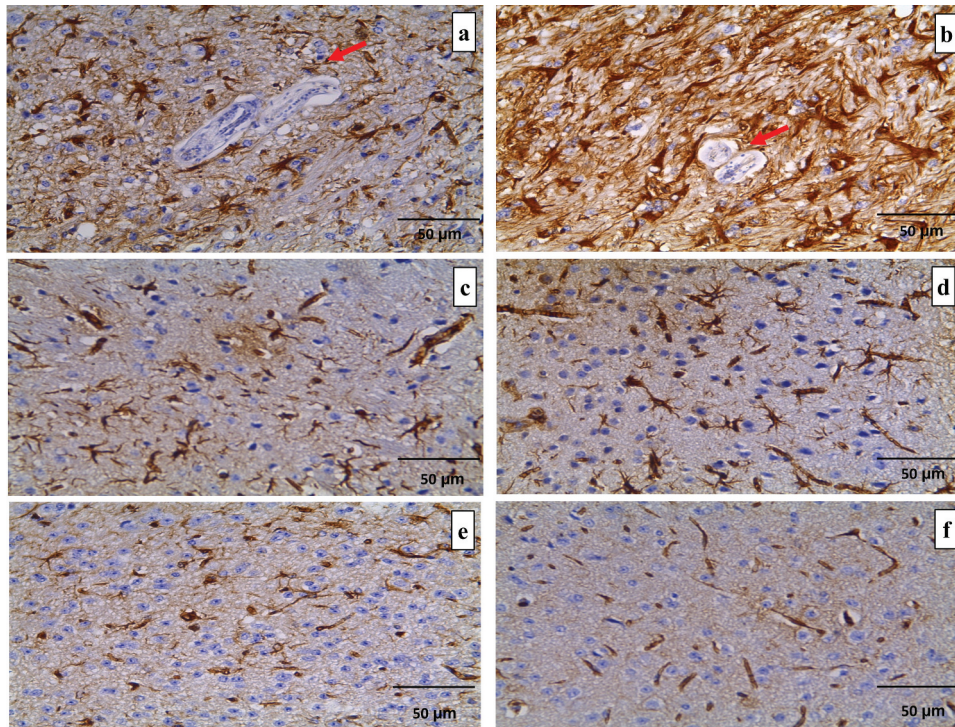


Figure 5. GFAP immunohistochemical staining of brain sections (immunoperoxidase $\times 400$): (a) early treatment control group showing moderate cytoplasmic expression in activated astrocytic cells in brain parenchyma around *T. canis* larva (red arrow) (+2). (b) late treatment control group showing strong cytoplasmic expression in activated astrocytic cells in the brain parenchyma (+3). (c) early albendazole group showing moderate cytoplasmic astrocytic expression (+2). (d) late albendazole group showing moderate cytoplasmic expression (+2). (e) early artemether group showing weak expression in activated astrocytes (+1) (f) late artemether group showing weak cytoplasmic expression in activated astrocytes (+1).

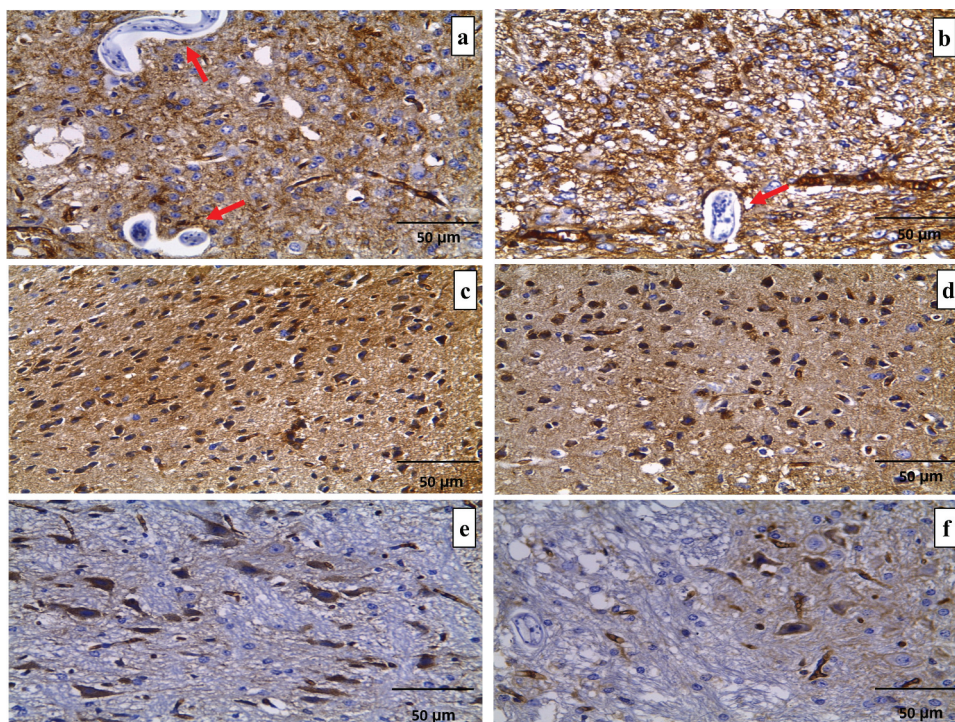


Figure 6. Caspase 3 immunohistochemical staining of brain sections (immunoperoxidase $\times 400$): (a) early treatment control group showing strong cytoplasmic expression in neuroglial cells (+3). (b) late treatment control group showing strong cytoplasmic expression in neuroglial cells (+3). (c) early albendazole group showing moderate cytoplasmic expression (+2). (d) late albendazole group showing moderate cytoplasmic expression (+2). (e) early artemether group showing weak expression in neuroglial cells (+1). (f) late artemether group showing weak expression in neuroglial cells (+1).

Table 3. Immunohistochemical expression of GFAP and caspase-3 in brain sections of studied groups. (n = 5).

Groups	GFAP				Caspase-3			
	0	+1	+2	+3	0	+1	+2	+3
Early treatment control (G IIa)	0	0	3	7	0	2	0	8
Early albendazole (G IIIa)	2	3	2	3	3	3	0	4
Early artemether (G IVa)	6	3	1	0	3	6	1	0
late treatment control (G IIb)	0	0	1	9	0	0	2	8
Late albendazole (G IIIb)	2	2	1	5	0	4	0	6
Late artemether (G IVb)	4	4	2	0	1	6	2	1
X ²			37.706				36.172	
P vaule			0.001*				0.002*	

*P < 0.05 (Significant).

n = number of studied mice in each group.

Chi-square (X²) test of significance.

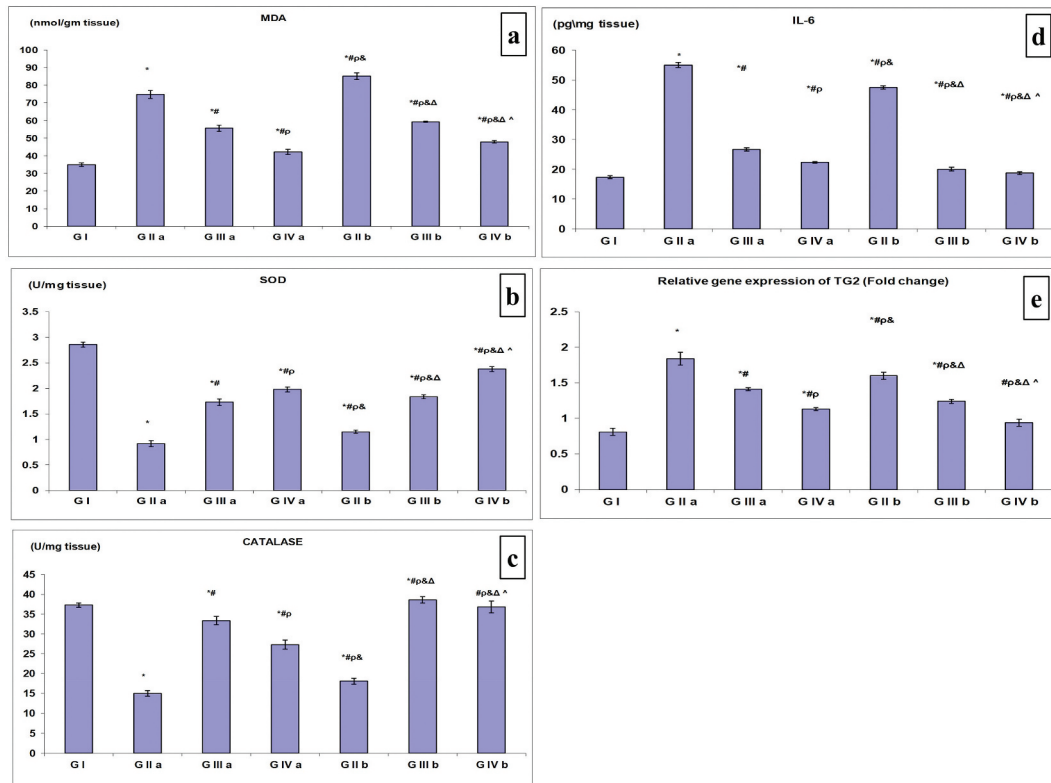


Figure 7. Bar charts showing comparisons between the studied groups as regards (a) the levels of MDA in the liver homogenates. (b) the levels of SOD in the liver homogenates. (c) the levels of catalase in the liver homogenates. (d) the levels of IL-6 in the liver homogenates. (e) relative gene expression of TG2 in liver tissue homogenates. * significant compared with G I, # significant compared with G II a, ρ significant compared with G III a, & significant compared with G IV a, Δ significant compared with G II b, and ^ significant compared with G III b.

study run consistently with the results of the earlier study by [88] who demonstrated that artemether possesses inhibitory actions against the NF-κB signaling pathway.

Apoptosis physiologically contributes to the equilibrium of neuronal cell development and cell death along with the regulation of neuroinflammation [89]. Substantial research has indicated the presence of a strong correlation between upregulated apoptosis and many neuroinflammatory or neurodegenerative diseases [89,90]. Furthermore, apoptosis is involved in the pathogenesis and sequelae of neurotoxocarisis [8]. Caspase-3 is most likely the best understood of the mammalian caspases in terms of its specificity and roles in apoptosis [91]. So as to assess the

apoptotic-signaling pathway of neuroglial cells, caspase-3 was evaluated. In this work, we detected that *T. canis* infection induced strong expression of caspase-3 in the brains of treatment control mice whether early or late. These results coincide with those of [92] who demonstrated that treatment of astrocytes with *T. canis* larval excretory-secretory antigens greatly enhanced caspase-3 activity. Additionally, we have shown that the administration of artemether treatment weakened the expression of caspase-3. Also, artemether outperformed albendazole at both time points post-infection in lowering caspase-3 expression. The results herein are coherent with those of [93] who demonstrated that the neuroprotective effects of artemether on cerebral ischemia injury are achieved

through reducing caspase-3 activation and the rate of cell apoptosis.

In light of the presented results, it may be assumed that in spite of the absence of inflammatory cellular infiltration in the brain of infected mice, the deleterious effects of *T. canis* infection appeared in the form of elevation of astrogliosis marker (GFAP), apoptosis marker (caspase-3) and mediator of inflammatory responses (NF- κ B). When comparing the outcomes of albendazole and artemether treatment in alleviating these effects, artemether was more effective than albendazole.

Regarding the effects of *T. canis* infection on the liver, the changes in the inflammatory status, oxidative stress, IL-6 and TG2 mRNA expression were explored. In the current research, histopathological examination of the livers of infected untreated mice showed the existence of granulomatous reactions around *T. canis* larvae. Granulomas were composed of aggregations of epithelioid cells, histiocytes, and eosinophils with deposition of fibrous tissue, especially in the late infected group. Similar findings were detected by [94]. They observed the presence of inflammatory responses in the form of eosinophils, neutrophils, polymorphonuclear cells, and lymphocytes in the liver parenchyma and around central veins.

In contrast, all treated groups demonstrated a diminished number and size of hepatic granulomas in early and late stages. Considering these findings, we supposed the potential anti-inflammatory mechanism of action of artemether. In a similar way, the results of the reduction in size and number of granulomas in the liver under the effect of artemether treatment were consistent with those reported by [95,96] who denoted reduction in both number and size of granulomas in hepatic schistosomiasis *mansoni* in artemether treated mice.

During *T. canis* infection, both the parasite and the host create an excessive amount of free radicals and reactive oxygen species [6,97]. Results of the oxidative stress biomarkers in this work showed significant increase of oxidative stress in the liver tissues of the treatment control group compared to the uninfected control group. Several previous studies agree with these findings [97–99]. The oxidative stress was down-regulated in all treated groups as demonstrated by the increase in the SOD and catalase levels and the decrease in the MDA levels. However, it didn't return to normal levels. The decrease in the oxidative stress in artemether treated groups than the treatment control group could be explained by the antiparasitic effect of artemether that led to reduction of the number of larvae reaching the tissues and consequently the resulting oxidative stress. However, the oxidative stress didn't reach the normal levels due to the well-known oxidative properties of artemether that share in its mechanism of action in killing parasites. These findings

are in line with those of [100–103] who reported that artemether possesses oxidative properties that help in killing adult and juvenile *S. japonicum* and *S. mansoni* worms.

In this study, we detected significant up-regulation in levels of IL-6 in the liver of the treatment control groups compared to the uninfected control group. Numerous earlier studies reported upregulation of IL-6 levels in *T. canis* infection [70,103–107]. IL-6 is a proinflammatory cytokine. In the liver, it is crucial for hepatocyte homeostasis, infection defense?. It also plays a role in metabolic function and liver regeneration [108]. Nevertheless, its persistent activation is detrimental to the liver [109]. In our study, levels of IL-6 decreased significantly in treated mice compared to the infected untreated control at both time points post-infection. Artemether treated groups showed significantly lower levels of IL-6 than albendazole treated groups. In line with our results [110], described decreased levels of IL-6 in the mice liver after artemether administration.

To provide insights into the underlying molecular host defense mechanisms against invading *T. canis* larvae, we investigated the effect of *T. canis* infection on the expression of TG2 gene in the liver. Transglutaminase 2 has a role in the control of inflammatory reactions and fibrosis in chronic hepatic diseases [111,112]. Furthermore, its activity is increased in response to several types of hepatic injury [113,114]. On the other hand, pharmacological inhibition of TG2 activity alleviated the resulting liver injury in lipopolysaccharides-induced sepsis mice [114]. Our study demonstrates for the first time, far as we can tell, a significant increase in TG2 gene expression in the livers of *T. canis* infected mice in comparison with the uninfected mice. A previous study by [60] recorded the role of the elevation of TG2 in neurodegenerative changes in the brain in the course of neurotoxocariasis. Our results showed that the expression of TG2 gene in the liver was significantly decreased in all the treated groups. Artemether treated mice showed the lowest relative TG2 mRNA expression. Also, this is the first time to report the reduction in TG2 expression in the liver tissues under the effect of artemether treatment.

Astonishingly, a probable link between TG2 and IL-6 was proposed. It was shown that TG2 activation is the way by which noninfectious stimuli activate the IL-6 signaling pathway leading to pulmonary epithelial cells fibrosis [115]. Depending on the findings described in the current study, pathological changes in the liver of *T. canis*-infected mice could be returned to the increased oxidative stress and the increased expression of both TG2 and IL-6. Also, it may be assumed that the effects of artemether in the reduction of expression of both TG2 and IL-6 could be the possible mechanisms by which it was able to reduce the pathological changes in the liver in response to *T. canis* infection.

Substantial research pointed to the probable relation between toxocariasis and bronchial asthma [116–118]. A previous study analyzed 17 studies utilizing a meta-analysis and systematic review and concluded that there was an upregulated risk of bronchial asthma in *Toxocara* seropositive children [119]. In the present work, we investigated the effects of *T. canis* infection on the lungs using histopathological examination with hematoxylin and eosin, and Masson's trichrome stains. The infected untreated mice exhibited dense inflammatory cellular infiltrate with patchy fibrosis. These findings increased in intensity in the late treatment control group than the early treatment control group. Similarly, a previous study by [120] found that *Toxocara* larvae in the lungs of infected mice induced insistent pulmonary inflammation, and airway hyperreactivity.

In contrast, in the current study, lung sections from the treated groups showed an evident reduction in the intensity of the inflammatory infiltration and fibrosis in comparison with the treatment control group. The best results were detected in sections from artemether treated groups. The ability of artemisinin derivatives to alleviate inflammation in different models of lung diseases was reported by many authors [121–125]. Additionally, our results demonstrated a significantly lower percentage area of collagen fibers in the groups that received artemether than the groups that received albendazole at both time points post-infection. These results concur with those of [126] who reported that artesunate attenuated bleomycin-induced pulmonary fibrosis. The antifibrotic effects of artemether were investigated by many researchers and they found numerous underlying mechanisms for these effects. Artemether has the ability to inhibit the proliferation and differentiation of myofibroblasts, extracellular matrix deposition, proangiogenic signaling, and angiogenesis, and downregulate profibrotic genes [127,128].

Conclusion

For the first time, this study demonstrated, novel promising effects of artemether against the pathological changes produced by *T. canis* infection in the brain, liver, and lungs of infected mice. Artemether succeeded in reducing *T. canis* larvae counts in the brain. The reduction in GFAP, caspase-3, and NF- κ B levels in the treated mice could be the possible mechanisms of artemether in alleviating brain injury. Besides, liver inflammation and fibrosis in the groups that received artemether were substantially reduced with a possible role of suppression of IL-6 and TG2 mRNA expression in these effects. Anti-inflammatory and anti-fibrotic properties of artemether appeared obviously in its effects on the lungs of infected animals. The effects of artemether were better than those achieved with albendazole. There was no obvious difference in the efficacy of artemether when administered either early or late in

the infection. Finally, our findings highlighted that artemether might be a promising therapy for *T. canis* infection and it could be a good substitution for albendazole. Consideration should be given to more research and controlled human trials of artemether in toxocariasis treatment.

Abbreviations

<i>T. canis</i>	<i>Toxocara canis</i>
CNS	Central nervous system
dpi	Day post-infection
H&E	Hematoxylin and eosin
GFAP	Glial fibrillary acidic protein
MDA	Malondialdehyde
SOD	Superoxide dismutase
NF- κ B	Nuclear factor kappa-light-chain-enhancer of activated B cells
IL-6	Interleukin 6
ELISA	Enzyme-linked immunosorbent assay
TG2	Transglutaminase 2
qRT-PCR	quantitative real-time Polymerase chain reaction


Disclosure statement

No potential conflict of interest was reported by the author(s).

Funding

The author(s) reported there is no funding associated with the work featured in this article.

ORCID

Dina I. Elgendy  <http://orcid.org/0000-0002-0070-6113>
 Rasha A. Elmahy  <http://orcid.org/0000-0003-0487-5659>
 Alaa Ibrahim Mohamed Amer  <http://orcid.org/0000-0001-7707-1796>
 Hoda A. Ibrahim  <http://orcid.org/0000-0002-8230-6761>
 Fotouh Rashed Mansour  <http://orcid.org/0000-0003-0847-4035>
 Amina M. Salama  <http://orcid.org/0000-0002-6754-6214>

Author contributions

Amina M. Salama and **Dina I. Elgendy** designed the study. **Rasha A. Elmahy**, **Amina M. Salama**, and **Dina I. Elgendy** performed the practical research. Biochemical tests were carried out by **Hoda A. Ibrahim**. **Alaa Ibrahim Mohamed Amer** performed histopathology analyses. **Dina I. Elgendy**, **Fotouh Rashed Mansour** and **Asmaa Fawzy Eltantawy** analyzed the whole data. **Dina I. Elgendy**, **Alaa Ibrahim Mohamed Amer**, **Hoda A. Ibrahim**, **Amina M. Salama**, and **Rasha A. Elmahy** wrote the original draft. All authors shared in reviewing and editing the manuscript. All authors approved the publication of the version.

References

- [1] Woodhall DM, Eberhard ML, Parise ME. Neglected parasitic infections in the United States: toxocariasis. *Am J Trop Med Hyg.* 2014 May;90(5):810–813. doi: [10.4269/ajtmh.13-0725](https://doi.org/10.4269/ajtmh.13-0725)
- [2] Kuenzli E, Neumayr A, Chaney M, et al. Toxocariasis-associated cardiac diseases—A systematic review of the literature. *Acta Trop.* 2016 Feb;154:107–120. doi: [10.1016/j.actatropica.2015.11.003](https://doi.org/10.1016/j.actatropica.2015.11.003)
- [3] El-Shazly AM, Abdel Baset SM, Kamal A, et al. Seroprevalence of human toxocariasis (visceral larva migrans). *J Egypt Soc Parasitol.* 2009 Dec;39(3):731–744.
- [4] Elshazly AM, Attia G, El-Ghareeb AS, et al. Clinical varieties of toxocariasis canis in children's hospital, Mansoura University: is it an underestimated problem? *J Egypt Soc Parasitol.* 2011 Aug;41(2):263–274.
- [5] Bayoumy AM, Atallah RB, Mohamed KAA, et al. Seroepidemiological evaluation of toxocariasis in Egyptian children suffering from recurrent urticaria. *Egypt J Hosp Med.* 2019;76(6):4262–4268. doi: [10.21608/ejhm.2019.43805](https://doi.org/10.21608/ejhm.2019.43805)
- [6] Gargili A, Demirci C, Kandil A, et al. In vivo inhibition of inducible nitric oxide and evaluation of the brain tissue damage induced by *Toxocara canis* larvae in experimentally infected mice. *Chin J Physiol.* 2004 Dec 31;47(4):189–196.
- [7] Othman AA, Abdel-Aleem GA, Saied EM, et al. Biochemical and immunopathological changes in experimental neurotoxocariasis. *Mol Biochem Parasitol.* 2010 Jul;172(1):1–8. doi: [10.1016/j.molbio para.2010.03.006](https://doi.org/10.1016/j.molbio para.2010.03.006)
- [8] Chou CM, Fan CK. Significant apoptosis rather autophagy predominates in astrocytes caused by *Toxocara canis* larval excretory-secretory antigens. *J Microbiol Immunol Infect.* 2020 Apr;53(2):250–258. doi: [10.1016/j.jmii.2018.06.006](https://doi.org/10.1016/j.jmii.2018.06.006)
- [9] Chen J, Zhou DH, Nisbet AJ, et al. Advances in molecular identification, taxonomy, genetic variation and diagnosis of *Toxocara* spp. *Infect Genet Evol.* 2012 Oct;12(7):1344–1348. doi: [10.1016/j.meegid.2012.04.019](https://doi.org/10.1016/j.meegid.2012.04.019)
- [10] Moreira GM, Telmo Pde L, Mendonça M, et al. Human toxocariasis: current advances in diagnostics, treatment, and interventions. *Trends Parasitol.* 2014 Sep;30(9):456–464. doi: [10.1016/j.pt.2014.07.003](https://doi.org/10.1016/j.pt.2014.07.003)
- [11] Figueiredo SD, Taddei JA, Menezes JJ, et al. Estudo clínico-epidemiológico da toxocaríase em população infantil [Clinical-epidemiological study of toxocariasis in a pediatric population]. *J Pediatr (Rio J).* 2005 Mar-Apr;81(2):126–132. doi: [10.2223/1317](https://doi.org/10.2223/1317)
- [12] Roldán WH, Espinoza YA, Atúnchar A, et al. Frequency of eosinophilia and risk factors and their association with *Toxocara* infection in schoolchildren during a health survey in the north of Lima, Peru. *Rev Inst Med Trop Sao Paulo.* 2008 Sep-Oct;50(5):273–278. doi: [10.1590/S0036-46652008000500005](https://doi.org/10.1590/S0036-46652008000500005)
- [13] Moreira-Silva SF, Rodrigues MG, Pimenta JL, et al. Toxocariasis of the central nervous system: with report of two cases. *Rev Soc Bras Med Trop.* 2004 Mar-Apr;37(2):169–174. doi: [10.1590/S0037-86822004000200011](https://doi.org/10.1590/S0037-86822004000200011)
- [14] Eberhardt O, Bialek R, Nägele T, et al. Eosinophilic meningomyelitis in toxocariasis: case report and review of the literature. *Clin Neurol Neurosur.* 2005 Aug;107(5):432–438. doi: [10.1016/j.clineuro.2004.10.003](https://doi.org/10.1016/j.clineuro.2004.10.003)
- [15] Fan CK, Holland CV, Loxton K, et al. Cerebral Toxocariasis: Silent Progression to Neurodegenerative Disorders? *Clin Microbiol Rev.* 2015 Jul;28(3):663–686. doi: [10.1128/CMR.00106-14](https://doi.org/10.1128/CMR.00106-14)
- [16] Sánchez SS, García HH, Nicoletti A. Clinical and magnetic resonance imaging findings of neurotoxocariasis. *Front Neurol.* 2018 Feb 8;9:53. doi: [10.3389/fneur.2018.00053](https://doi.org/10.3389/fneur.2018.00053)
- [17] Janecek E, Waindak P, Bankstahl M, et al. Abnormal neurobehaviour and impaired memory function as a consequence of *Toxocara canis*- as well as *Toxocara cati*-induced neurotoxocarosis. *PLoS Negl Trop Dis.* 2017 May 8;11(5):e0005594. doi: [10.1371/journal.pntd.0005594](https://doi.org/10.1371/journal.pntd.0005594)
- [18] El-Sayed NM, Ramadan ME. Toxocariasis in children: an update on clinical manifestations, diagnosis, and treatment. *J Pediatr Infect Dis.* 2017;12(4):222–227. doi: [10.1055/s-0037-1603496](https://doi.org/10.1055/s-0037-1603496)
- [19] Mata-Santos T, Pinto NF, Mata-Santos HA, et al. Anthelmintic Activity Of Lapachol, β -Lapachone And Its Derivatives Against *Toxocara canis* Larvae. *Rev Inst Med Trop Sao Paulo.* 2015 May-Jun;57(3):197–204. doi: [10.1590/S0036-46652015000300003](https://doi.org/10.1590/S0036-46652015000300003)
- [20] Despommier D. Toxocariasis: clinical aspects, epidemiology, medical ecology, and molecular aspects. *Clin Microbiol Rev.* 2003 Apr;16(2):265–272. doi: [10.1128/CMR.16.2.265-272.2003](https://doi.org/10.1128/CMR.16.2.265-272.2003)
- [21] Daniel-Mwambete K, Torrado S, Cuesta-Bandera C, et al. The effect of solubilization on the oral bioavailability of three benzimidazole carbamate drugs. *Int J Pharm.* 2004 Mar 19;272(1–2):29–36. doi: [10.1016/j.ijpharm.2003.11.030](https://doi.org/10.1016/j.ijpharm.2003.11.030)
- [22] Rigter IM, Schipper HG, Koopmans RP, et al. Relative bioavailability of three newly developed albendazole formulations: a randomized crossover study with healthy volunteers. *Antimicrob Agents Chemother.* 2004 Mar;48(3):1051–1054. doi: [10.1128/AAC.48.3.1051-1054.2004](https://doi.org/10.1128/AAC.48.3.1051-1054.2004)
- [23] Dayan AD. Albendazole, mebendazole and praziquantel. Review of non-clinical toxicity and pharmacokinetics. *Acta Trop.* 2003 May;86(2–3):141–159. doi: [10.1016/S0001-706X\(03\)00031-7](https://doi.org/10.1016/S0001-706X(03)00031-7)
- [24] Musa D, Senocak G, Borazan G, et al. Effects of *Nigella sativa* and albendazole alone and in combination in *Toxocara canis* infected mice. *J Pak Med Assoc.* 2011 Sep;61(9):866–870.
- [25] Deshayes S, Bonhomme J, de La Blanchardière A. Neurotoxocariasis: a systematic literature review. *Infection.* 2016 Oct;44(5):565–574. doi: [10.1007/s15010-016-0889-8](https://doi.org/10.1007/s15010-016-0889-8)
- [26] Kroten A, Toczyłowski K, Oldak E, et al. Toxocarosis in children: poor hygiene habits and contact with dogs is related to longer treatment. *Parasitol Res.* 2018 May;117(5):1513–1519. doi: [10.1007/s00436-018-5833-7](https://doi.org/10.1007/s00436-018-5833-7)
- [27] Ma G, Holland CV, Wang T, et al. Human toxocariasis. *Lancet Infect Dis.* 2018 Jan;18(1):e14–e24. doi: [10.1016/S1473-3099\(17\)30331-6](https://doi.org/10.1016/S1473-3099(17)30331-6)
- [28] Horton RJ. Albendazole in treatment of human cystic echinococcosis: 12 years of experience. *Acta Trop.* 1997 Apr 1;64(1–2):79–93.
- [29] Horton J. Albendazole: a review of anthelmintic efficacy and safety in humans. *Parasitology.* 2000;121 Suppl(S1): S113–132. doi: [10.1017/S0031182000007290](https://doi.org/10.1017/S0031182000007290)
- [30] Choi GY, Yang HW, Cho SH, et al. Acute drug-induced hepatitis caused by albendazole. *J Korean Med Sci.* 2008 Oct;23(5):903–905. doi: [10.3346/jkms.2008.23.5.903](https://doi.org/10.3346/jkms.2008.23.5.903)

- [31] Tas A, Köklü S, Celik H. Loss of body hair as a side effect of albendazole. *Wien Klin Wochenschr.* 2012 Mar;124(5–6):220. doi: [10.1007/s00508-011-0112-y](https://doi.org/10.1007/s00508-011-0112-y)
- [32] Marin Zuluaga JI, Marin Castro AE, Perez Cadavid JC, et al. Albendazole-induced granulomatous hepatitis: a case report. *J Med Case Rep.* 2013 Jul 26;7(1):201. doi: [10.1186/1752-1947-7-201](https://doi.org/10.1186/1752-1947-7-201)
- [33] Haynes RK. From artemisinin to new artemisinin anti-malarials: biosynthesis, extraction, old and new derivatives, stereochemistry and medicinal chemistry requirements. *Curr Top Med Chem.* 2006;6(5):509–537. doi: [10.2174/156802606776743129](https://doi.org/10.2174/156802606776743129)
- [34] White NJ. The treatment of malaria. *N Engl J Med.* 1996 Sep 12;335(11):800–806.
- [35] Bunnag D, Viravan C, Looareesuwan S, et al. Clinical trial of artesunate and artemether on multidrug resistant falciparum malaria in Thailand. A preliminary report. *Southeast Asian J Trop Med Public Health.* 1991 Sep;22(3):380–385.
- [36] Adekunle AS, Falade CO, Agbedana EO, et al. Assessment of side effects of administration of artemether in humans. *BiolMed.* 2009;1(3):15–19..
- [37] Liu YX, Wu W, Liang YJ, et al. New uses for old drugs: the tale of artemisinin derivatives in the elimination of schistosomiasis japonica in China. *Molecules.* 2014 Sep 19;19(9):15058–15074.
- [38] Keiser J, Utzinger J. Artemisinins and synthetic trioxolanes in the treatment of helminth infections. *Curr Opin Infect Dis.* 2007 Dec;20(6):605–612. doi: [10.1097/QCO.0b013e3282f19ec4](https://doi.org/10.1097/QCO.0b013e3282f19ec4)
- [39] Shalaby HA, Abdel-Shafy S, Abdel-Rahman KA, et al. Comparative in vitro effect of artemether and albendazole on adult *Toxocara canis*. *Parasitol Res.* 2009 Oct;105(4):967–976. doi: [10.1007/s00436-009-1479-9](https://doi.org/10.1007/s00436-009-1479-9)
- [40] Derda M, Hadaś E, Cholewiński M, et al. As a plant with potential use in the treatment of acanthamoebiasis. *Parasitol Res.* 2016 Apr;115(4):1635–1639. doi: [10.1007/s00436-016-4902-z](https://doi.org/10.1007/s00436-016-4902-z)
- [41] Crespo-Ortiz MP, Wei MQ. Antitumor activity of artemisinin and its derivatives: from a well-known antimalarial agent to a potential anticancer drug. *J Biomed Biotechnol.* 2012;2012:247597. doi: [10.1155/2012/247597](https://doi.org/10.1155/2012/247597)
- [42] Appalasaamy S, Lo KY, Ch'ng SJ, et al. Antimicrobial activity of artemisinin and precursor derived from in vitro plantlets of *Artemisia annua* L. *Biomed Res Int.* 2014;2014:215872. doi: [10.1155/2014/215872](https://doi.org/10.1155/2014/215872)
- [43] Shi C, Li H, Yang Y, et al. Anti-inflammatory and immunoregulatory functions of artemisinin and its derivatives. *Mediators Inflamm.* 2015;2015:435713. doi: [10.1155/2015/435713](https://doi.org/10.1155/2015/435713)
- [44] Li S, Zhao X, Lazarovici P, et al. Artemether Activation of AMPK/GSK3 β (ser9)/Nrf2 Signaling Confers Neuroprotection towards β -Amyloid-Induced Neurotoxicity in 3xTg Alzheimer's Mouse Model. *Oxid Med Cell Longev.* 2019 Nov 21;2019:1862437. doi: [10.1155/2019/1862437](https://doi.org/10.1155/2019/1862437)
- [45] Abou Rayia DM, Saad AE, Ashour DS, et al. Implication of artemisinin nematocidal activity on experimental trichinellosis: In vitro and in vivo studies. *Parasitol Int.* 2017 Apr;66(2):56–63. doi: [10.1016/j.parint.2016.11.012](https://doi.org/10.1016/j.parint.2016.11.012)
- [46] Nassef NA, El-Kersh WM, El-Nahas NS, et al. Parasitological, histopathological, and immunohistochemical assessment of nitric oxide synthase inhibitor: aminoguanidine versus albendazole in the treatment of experimental murine toxocarosis. *Menoufia Med J.* 2014;27(1):103.. doi: [10.4103/1110-2098.132778](https://doi.org/10.4103/1110-2098.132778)
- [47] Kayes SG, Oaks JA. Effect of inoculum size and length of infection on the distribution of *Toxocara canis* larvae in the mouse. *Am J Trop Med Hyg.* 1976 Jul;25(4):573–580. doi: [10.4269/ajtmh.1976.25.573](https://doi.org/10.4269/ajtmh.1976.25.573)
- [48] Faz-López B, Ledesma-Soto Y, Romero-Sánchez Y, et al. Signal transducer and activator of transcription factor 6 signaling contributes to control host lung pathology but favors susceptibility against *Toxocara canis* infection. *Biomed Res Int.* 2013;2013:696343. doi: [10.1155/2013/696343](https://doi.org/10.1155/2013/696343)
- [49] Tanabe N, McDonough JE, Vasilescu DM, et al. Pathology of idiopathic pulmonary fibrosis assessed by a combination of microcomputed tomography, histology, and immunohistochemistry. *Am J Pathol.* 2020 Dec;190(12):2427–2435. doi: [10.1016/j.ajpath.2020.09.001](https://doi.org/10.1016/j.ajpath.2020.09.001)
- [50] Ozawa A, Sakaue M. New decolorization method produces more information from tissue sections stained with hematoxylin and eosin stain and Masson-trichrome stain. *Ann Anat.* 2020 Jan;227:151431. doi: [10.1016/j.aanat.2019.151431](https://doi.org/10.1016/j.aanat.2019.151431)
- [51] Shi SR, Shi Y, Taylor CR. Antigen retrieval immunohistochemistry: review and future prospects in research and diagnosis over two decades. *J Histochem Cytochem.* 2011 Jan;59(1):13–32. doi: [10.1369/jhc.2010.957191](https://doi.org/10.1369/jhc.2010.957191)
- [52] Reyaz N, Tayyab M, Khan SA, et al. Correlation of glial fibrillary acidic protein (GFAP) with grading of the neuroglial tumours. *J Coll Physicians Surg Pak.* 2005 Aug;15(8):472–475.
- [53] Saraswati S, Agrawal SS, Alhaider AA. Ursolic acid inhibits tumor angiogenesis and induces apoptosis through mitochondrial-dependent pathway in Ehrlich ascites carcinoma tumor. *Chem Biol Interact.* 2013 Nov 25;206(2):153–165.
- [54] Oh K, Moon HG, Lee DS, et al. Tissue transglutaminase-interleukin-6 axis facilitates peritoneal tumor spreading and metastasis of human ovarian cancer cells. *Lab Anim Res.* 2015 Dec;31(4):188–197. doi: [10.5625/lar.2015.31.4.188](https://doi.org/10.5625/lar.2015.31.4.188)
- [55] Schoenardie ER, Scaini CJ, Pepe MS, et al. Vertical transmission of *Toxocara canis* in successive generations of mice. *Rev Bras Parasitol Vet.* 2013 Oct-Dec;22(4):623–626. doi: [10.1590/S1984-29612013000400030](https://doi.org/10.1590/S1984-29612013000400030)
- [56] Strube C, Heuer L, Janecek E. *Toxocara* spp. infections in paratenic hosts. *Vet Parasitol.* 2013 Apr 15;193(4):375–389.
- [57] Abo-Shehada MN, Herbert IV. The migration of larval *Toxocara canis* in mice. II. Post-intestinal migration in primary infections. *Vet Parasitol.* 1984 Dec;17(1):75–83. doi: [10.1016/0304-4017\(84\)90066-9](https://doi.org/10.1016/0304-4017(84)90066-9)
- [58] Janecek E, Beineke A, Schnieder T, et al. Neurotoxocarosis: marked preference of *Toxocara canis* for the cerebrum and *T. cati* for the cerebellum in the paratenic model host mouse. *Parasites Vectors.* 2014 Apr 22;7(1):194. doi: [10.1186/1756-3305-7-194](https://doi.org/10.1186/1756-3305-7-194)
- [59] Lai SC, Chen KM, Chen HC, et al. Induction of matrix metalloproteinase-9 in mice during *Toxocara canis* larvae migration. *Parasitol Res.* 2005 Feb;95(3):193–200. doi: [10.1007/s00436-004-1271-9](https://doi.org/10.1007/s00436-004-1271-9)
- [60] Chou CM, Lee YL, Liao CW, et al. Enhanced expressions of neurodegeneration-associated factors, UPS impairment, and excess A β accumulation in the hippocampus of mice with persistent cerebral toxocarosis. *Parasites Vectors.* 2017 Dec 22;10(1):620. doi: [10.1186/s13071-017-2578-6](https://doi.org/10.1186/s13071-017-2578-6)

- [61] Holland CV, Hamilton CM. The significance of cerebral toxocariasis: a model system for exploring the link between brain involvement, behaviour and the immune response. *J Exp Biol.* 2013 Jan 1;216(Pt 1):78–83.
- [62] Xiao S, Tanner M, N'Goran EK, et al. Recent investigations of artemether, a novel agent for the prevention of schistosomiasis japonica, mansoni and haematobia. *Acta Trop.* 2002 May;82(2):175–181. doi: [10.1016/S0001-706X\(02\)00009-8](https://doi.org/10.1016/S0001-706X(02)00009-8)
- [63] Wang W, Li TY, Ji Y, et al. Efficacy of artemether and artesunate in mice infected with praziquantel non-susceptible isolate of *Schistosoma japonicum*. *Parasitol Res.* 2014 Mar;113(3):925–931. doi: [10.1007/s00436-013-3724-5](https://doi.org/10.1007/s00436-013-3724-5)
- [64] Meshnick SR. Artemisinin antimalarials: mechanisms of action and resistance. *Med Trop.* 1998 Mar;58(3 Suppl):13–17.
- [65] Meshnick SR. Artemisinin and its derivatives. In: Rosenthal PJ, editor. *Antimalarial chemotherapy. Infectious disease.* Totowa, NJ: Humana Press; 2001. doi:[10.1007/978-1-59259-111-4_10](https://doi.org/10.1007/978-1-59259-111-4_10)
- [66] Bridgford JL, Xie SC, Cobbold SA, et al. Artemisinin kills malaria parasites by damaging proteins and inhibiting the proteasome. *Nat Commun.* 2018 Aug;9(1):3801. doi: [10.1038/s41467-018-06221-1](https://doi.org/10.1038/s41467-018-06221-1)
- [67] Liao CW, Fan CK, Kao TC, et al. Brain injury-associated biomarkers of TGF-beta1, S100B, GFAP, NF-L, tTG, AbetaPP, and tau were concomitantly enhanced and the UPS was impaired during acute brain injury caused by *Toxocara canis* in mice. *BMC Infect Dis.* 2008 Jun 24;8(1):84. doi: [10.1186/1471-2334-8-84](https://doi.org/10.1186/1471-2334-8-84)
- [68] Eid MM, El-Kowrany SI, Othman AA, et al. Immunopathological changes in the brain of immunosuppressed mice experimentally infected with *Toxocara canis*. *Korean J Parasitol.* 2015 Feb;53(1):51–58. doi: [10.3347/kjp.2015.53.1.51](https://doi.org/10.3347/kjp.2015.53.1.51)
- [69] Springer A, Heuer L, Janeczek-Erfurth E, et al. Histopathological characterization of *Toxocara canis*- and *T. cati*-induced neurotoxocarosis in the mouse model. *Parasitol Res.* 2019 Sep;118(9):2591–2600. doi: [10.1007/s00436-019-06395-7](https://doi.org/10.1007/s00436-019-06395-7)
- [70] Waindok P, Strube C. Neuroinvasion of *Toxocara canis*- and *T. cati*-larvae mediates dynamic changes in brain cytokine and chemokine profile. *J Neuroinflammation.* 2019 Jul 17;16(1):147.
- [71] Clark RS, Kochanek PM, Watkins SC, et al. Caspase-3 mediated neuronal death after traumatic brain injury in rats. *J Neurochem.* 2000 Feb;74(2):740–753. doi: [10.1046/j.1471-4159.2000.740740.x](https://doi.org/10.1046/j.1471-4159.2000.740740.x)
- [72] D'Amelio M, Sheng M, Cecconi F. Caspase-3 in the central nervous system: beyond apoptosis. *Trends Neurosci.* 2012 Nov;35(11):700–709. doi: [10.1016/j.tins.2012.06.004](https://doi.org/10.1016/j.tins.2012.06.004)
- [73] Okonkwo DO, Yue JK, Puccio AM, et al. Transforming research and clinical knowledge in traumatic brain injury (TRACK-TBI) investigators. GFAP-BDP as an acute diagnostic marker in traumatic brain injury: results from the prospective transforming research and clinical knowledge in traumatic brain injury study. *J Neurotrauma.* 2013 Sep 1;30(17):1490–1497.
- [74] Li YX, Sibon OCM, Dijkers PF. Inhibition of NF-κB in astrocytes is sufficient to delay neurodegeneration induced by proteotoxicity in neurons. *J Neuroinflammation.* 2018 Sep 11;15(1):261.
- [75] Vainchtein ID, Molofsky AV. Astrocytes and Microglia: in sickness and in health. *Trends Neurosci.* 2020 Mar;43(3):144–154. doi: [10.1016/j.tins.2020.01.003](https://doi.org/10.1016/j.tins.2020.01.003)
- [76] Sofroniew MV, Vinters HV. Astrocytes: biology and pathology. *Acta Neuropathol.* 2010 Jan;119(1):7–35. doi: [10.1007/s00401-009-0619-8](https://doi.org/10.1007/s00401-009-0619-8)
- [77] Mengying Z, Yiyue X, Tong P, et al. Apoptosis and necroptosis of mouse hippocampal and parenchymal astrocytes, microglia and neurons caused by *Angiostrongylus cantonensis* infection. *Parasites Vectors.* 2017 Dec 19;10(1):611. doi: [10.1186/s13071-017-2565-y](https://doi.org/10.1186/s13071-017-2565-y)
- [78] Silver J, Miller JH. Regeneration beyond the glial scar. *Nat Rev Neurosci.* 2004 Feb;5(2):146–156. doi: [10.1038/nrn1326](https://doi.org/10.1038/nrn1326)
- [79] Kwon HS, Koh SH. Neuroinflammation in neurodegenerative disorders: the roles of microglia and astrocytes. *Transl Neurodegener.* 2020;9:1–12. doi: [10.1186/s40035-020-00221-2](https://doi.org/10.1186/s40035-020-00221-2)
- [80] Abbott NJ, Rönnbäck L, Hansson E. Astrocyte-endothelial interactions at the blood-brain barrier. *Nat Rev Neurosci.* 2006 Jan;7(1):41–53. doi: [10.1038/nrn1824](https://doi.org/10.1038/nrn1824)
- [81] Abdelhak A, Foschi M, Abu-Rumeileh S, et al. Blood GFAP as an emerging biomarker in brain and spinal cord disorders. *Nat Rev Neurol.* 2022 Mar;18(3):158–172. doi: [10.1038/s41582-021-00616-3](https://doi.org/10.1038/s41582-021-00616-3)
- [82] Edagha IA, Peter AI, Aquaisua AN. Histopathological effect of *Nauclea latifolia* ethanolic leaf extract and artemether/lumefantrine on the hippocampus of *P. berghei*-infected mice. *Int J Brain Cognitive Sci.* 2017;6:9–16..
- [83] O'Neill LA, Kaltschmidt C. NF-kappa B: a crucial transcription factor for glial and neuronal cell function. *Trends Neurosci.* 1997 Jun;20(6):252–258. doi: [10.1016/S0166-2236\(96\)01035-1](https://doi.org/10.1016/S0166-2236(96)01035-1)
- [84] Mattson MP, Camandola S. NF-kappaB in neuronal plasticity and neurodegenerative disorders. *J Clin Invest.* 2001 Feb;107(3):247–254. doi: [10.1172/JCI11916](https://doi.org/10.1172/JCI11916)
- [85] Downer EJ, Johnston DG, Lynch MA. Differential role of Dok1 and Dok2 in TLR2-induced inflammatory signaling in glia. *Mol Cell Neurosci.* 2013 Sep;56:148–158. doi: [10.1016/j.mcn.2013.04.007](https://doi.org/10.1016/j.mcn.2013.04.007)
- [86] Elgendy DI, Othman A, Saied E, et al. Assessment of neuroinflammatory and neurodegenerative alterations in the brain in a mouse model of visceral larva migrans. *J Egypt Soc Parasitol.* 2020;50(3):467–476.. doi: [10.21608/jesp.2020.130833](https://doi.org/10.21608/jesp.2020.130833)
- [87] Li F, Li XL, Chen SJ, et al. Excretory/Secretory proteins of adult *Toxocara canis* induce changes in the expression of proteins involved in the NOD1-RIP2-NF-κB pathway and modulate cytokine production in mouse macrophages. *Exp Parasitol.* 2021 Oct;229:108152.
- [88] Okorji UP, Velagapudi R, El-Bakoush A, et al. Antimalarial drug artemether inhibits Neuroinflammation in BV2 microglia through Nrf2-dependent mechanisms. *Mol Neurobiol.* 2016 Nov;53(9):6426–6443. doi: [10.1007/s12035-015-9543-1](https://doi.org/10.1007/s12035-015-9543-1)
- [89] Ghavami S, Shojaei S, Yeganeh B, et al. Autophagy and apoptosis dysfunction in neurodegenerative disorders. *Prog Neurobiol.* 2014 Jan;112:24–49.
- [90] Menzies FM, Fleming A, Rubinsztein DC. Compromised autophagy and neurodegenerative diseases. *Nat Rev Neurosci.* 2015 Jun;16(6):345–457. doi: [10.1038/nrn3961](https://doi.org/10.1038/nrn3961)
- [91] Porter AG, Jänicke RU. Emerging roles of caspase-3 in apoptosis. *Cell Death Differ.* 1999 Feb;6(2):99–104. doi: [10.1038/sj.cdd.4400476](https://doi.org/10.1038/sj.cdd.4400476)
- [92] Beshay EVN, El-Refai SA, Sadek GS, et al. Mesenchymal stem cells combined with albendazole as a novel therapeutic approach for experimental neurotoxocarosis.

- Parasitology. 2020 Jun;147(7):799–809. doi: [10.1017/S003118202000044X](https://doi.org/10.1017/S003118202000044X)
- [93] Li S, Peng T, Zhao X, et al. Artemether confers neuro-protection on cerebral ischemic injury through stimulation of the Erk1/2-P90rsk-CREB signaling pathway. *Redox Biol.* 2021 Oct;46:102069.
- [94] Resende NM, Gazzinelli-Guimarães PH, Barbosa FS, et al. New insights into the immunopathology of early *Toxocara canis* infection in mice. *Parasites Vectors.* 2015 Jul 2;8(1):354.
- [95] Botros SS, Mahmoud MR, Moussa MM, et al. Immunohistopathological and biochemical changes in *Schistosoma mansoni*-infected mice treated with artemether. *J Infect.* 2007 Nov;55(5):470–477. doi: [10.1016/j.jinf.2007.07.022](https://doi.org/10.1016/j.jinf.2007.07.022)
- [96] Madbouly NA, Shalash IR, El Deeb SO, et al. Effect of artemether on cytokine profile and egg induced pathology in murine schistosomiasis mansoni. *J Adv Res.* 2015 Nov;6(6):851–857. doi: [10.1016/j.jare.2014.07.003](https://doi.org/10.1016/j.jare.2014.07.003)
- [97] Demirci C, Gargili A, Kandil A, et al. Inhibition of inducible nitric oxide synthase in murine visceral larva migrans: effects on lung and liver damage. *Chin J Physiol.* 2006 Dec 31;49(6):326–334.
- [98] Yarsan E, Ç A, Ayçiçek H, et al. Effects of albendazole treatment on haematological and biochemical parameters in healthy and *Toxocara canis* infected mice. *Turk J Vet Anim Sci.* 2003;27(5):1057–1063..
- [99] Moawad MA, Amin MM, Hafez EN. Role of ionizing radiation on controlling kidney changes in experimental infection with *Toxocara canis*. *AVMJ.* 2015;61(147):87–94..
- [100] Sayiner S, Altaş M, Camkerten G, et al. Kidney tissue selenium levels of *Toxocara canis* infected mice given *Nigella sativa*. *J VetBio Sci Tech.* 2021;6(3):278–283.. doi: [10.31797/vetbio.977962](https://doi.org/10.31797/vetbio.977962)
- [101] Xiao SH, You JQ, Gao HF, et al. *Schistosoma japonicum*: effect of artemether on glutathione S-transferase and superoxide dismutase. *Exp Parasitol.* 2002 Sep;102(1):38–45. doi: [10.1016/S0014-4894\(02\)00145-5](https://doi.org/10.1016/S0014-4894(02)00145-5)
- [102] El-Bassiouni EA, Helmy MH, Saad El, et al. Modulation of the antioxidant defence in different developmental stages of *Schistosoma mansoni* by praziquantel and artemether. *Br J Biomed Sci.* 2007;64(4):168–174. doi: [10.1080/09674845.2007.11732782](https://doi.org/10.1080/09674845.2007.11732782)
- [103] El-Lakkany NM, Seif El-Din SH. Haemin enhances the in vivo efficacy of artemether against juvenile and adult *Schistosoma mansoni* in mice. *Parasitol Res.* 2013 May;112(5):2005–2015. doi: [10.1007/s00436-013-3358-7](https://doi.org/10.1007/s00436-013-3358-7)
- [104] Pecinali NR, Gomes RN, Amendoeira FC, et al. Influence of murine *Toxocara canis* infection on plasma and bronchoalveolar lavage fluid eosinophil numbers and its correlation with cytokine levels. *Vet Parasitol.* 2005 Nov 25;134(1–2):121–130.
- [105] Hamilton CM, Brandes S, Holland CV, et al. Cytokine expression in the brains of *Toxocara canis*-infected mice. *Parasite Immunol.* 2008 Mar;30(3):181–185. doi: [10.1111/j.1365-3024.2007.01002.x](https://doi.org/10.1111/j.1365-3024.2007.01002.x)
- [106] Cheng Y, Li J, Peng J. Study on variable IL–6 and IL–8 levels in the serum of SD rats infected with *Toxocara canis*. *Zhongguo Bingyuan Shengwuxue Zazhi/Journal Of Pathogen Biology.* 2010;5(8):601–603..
- [107] Długosz E, Wasyl K, Klockiewicz M, et al. *Toxocara canis* mucins among other excretory-secretory antigens induce in vitro secretion of cytokines by mouse splenocytes. *Parasitol Res.* 2015 Sep;114(9):3365–3371. doi: [10.1007/s00436-015-4561-5](https://doi.org/10.1007/s00436-015-4561-5)
- [108] Michalopoulos GK. Liver regeneration after partial hepatectomy: critical analysis of mechanistic dilemmas. *Am J Pathol.* 2010 Jan;176(1):2–13. doi: [10.2353/ajpath.2010.090675](https://doi.org/10.2353/ajpath.2010.090675)
- [109] Schmidt-Arras D, Rose-John S. IL-6 pathway in the liver: from physiopathology to therapy. *J Hepatol.* 2016 Jun;64(6):1403–1415. doi: [10.1016/j.jhep.2016.02.004](https://doi.org/10.1016/j.jhep.2016.02.004)
- [110] Fu W, Ma Y, Li L, et al. Artemether Regulates Metaflammation to Improve Glycolipid Metabolism in db/db Mice. *Diabetes Metab Syndr Obes.* 2020 May 19;13:1703–1713. doi: [10.2147/DMSO.S240786](https://doi.org/10.2147/DMSO.S240786).
- [111] Elli L, Bergamini CM, Bardella MT, et al. Transglutaminases in inflammation and fibrosis of the gastrointestinal tract and the liver. *Dig Liver Dis.* 2009 Aug;41(8):541–550. doi: [10.1016/j.dld.2008.12.095](https://doi.org/10.1016/j.dld.2008.12.095)
- [112] Jeong EM, Son YH, Choi Y, et al. Transglutaminase 2 is dispensable but required for the survival of mice in dextran sulfate sodium-induced colitis. *Exp Mol Med.* 2016 Nov 4;48(11):e267. doi: [10.1038/emm.2016.95](https://doi.org/10.1038/emm.2016.95)
- [113] Tatsukawa H, Fukaya Y, Frampton G, et al. Role of transglutaminase 2 in liver injury via cross-linking and silencing of transcription factor Sp1. *Gastroenterology.* 2009 May;136(5):1783–95.e10. doi: [10.1053/j.gastro.2009.01.007](https://doi.org/10.1053/j.gastro.2009.01.007)
- [114] Su T, Qin XY, Furutani Y, et al. Imaging of the ex vivo transglutaminase activity in liver macrophages of sepsis mice. *Anal Biochem.* 2020 May 15;597:113654.
- [115] Oh K, Park HB, Byoun OJ, et al. Epithelial transglutaminase 2 is needed for T cell interleukin-17 production and subsequent pulmonary inflammation and fibrosis in bleomycin-treated mice. *J Exp Med.* 2011 Aug 1;208(8):1707–1719. doi: [10.1084/jem.20101457](https://doi.org/10.1084/jem.20101457)
- [116] Kanobana K, Vereecken K, Junco Diaz R, et al. *Toxocara* seropositivity, atopy and asthma: a study in Cuban schoolchildren. *Trop Med Int Health.* 2013 Apr;18(4):403–406. doi: [10.1111/tmi.12073](https://doi.org/10.1111/tmi.12073)
- [117] Li L, Gao W, Yang X, et al. Asthma and toxocariasis. *Ann Allergy Asthma Immunol.* 2014 Aug;113(2):187–192. doi: [10.1016/j.anai.2014.05.016](https://doi.org/10.1016/j.anai.2014.05.016)
- [118] Khozime A, Mirsadraee M, Borji H. *Toxocara* sero-prevalence and its relationship with allergic asthma in asthmatic patients in north-eastern Iran. *J Helminthol.* 2019 Nov;93(6):677–680. doi: [10.1017/S0022149X1800086X](https://doi.org/10.1017/S0022149X1800086X)
- [119] Aghaei S, Riahi SM, Rostami A, et al. *Toxocara* spp. infection and risk of childhood asthma: a systematic review and meta-analysis. *Acta Trop.* 2018 Jun;182:298–304.
- [120] Pinelli E, Brandes S, Dormans J, et al. Infection with the roundworm *Toxocara canis* leads to exacerbation of experimental allergic airway inflammation. *Clin Exp Allergy.* 2008 Apr;38(4):649–658. doi: [10.1111/j.1365-2222.2007.02908.x](https://doi.org/10.1111/j.1365-2222.2007.02908.x)
- [121] Cheng C, Ho WE, Goh FY, et al. Anti-malarial drug artesunate attenuates experimental allergic asthma via inhibition of the phosphoinositide 3-kinase/Akt pathway. *PLoS One.* 2011;6(6):e20932. doi: [10.1371/journal.pone.0020932](https://doi.org/10.1371/journal.pone.0020932)
- [122] Ho WE, Cheng C, Peh HY, et al. Anti-malarial drug artesunate ameliorates oxidative lung damage in experimental allergic asthma. *Free Radic Biol Med.* 2012 Aug 1;53(3):498–507. doi: [10.1016/j.freeradbiomed.2012.05.021](https://doi.org/10.1016/j.freeradbiomed.2012.05.021)
- [123] Wei M, Xie X, Chu X, et al. Dihydroartemisinin suppresses ovalbumin-induced airway inflammation in a mouse allergic asthma model. *Immunopharmacol*

- Immunotoxicol. 2013 Jun;35(3):382–389. doi: [10.3109/08923973.2013.785559](https://doi.org/10.3109/08923973.2013.785559)
- [124] Luo QZ, Lin JT, Li H, et al. Effects of artesunate on cigarette smoke-induced lung oxidative damage in mice and the expression of Nrf2 and the possible mechanism. *Zhonghua Yi Xue Za Zhi*. 2016 Mar 29;96(12):960–965.
- [125] Cao TH, Jin SG, Fei DS, et al. Artesunate Protects Against Sepsis-Induced Lung Injury Via Heme Oxygenase-1 Modulation. *Inflammation*. 2016 Apr;39(2):651–662. doi: [10.1007/s10753-015-0290-2](https://doi.org/10.1007/s10753-015-0290-2)
- [126] Wang Y, Huang G, Mo B, et al. Artesunate modulates expression of matrix metalloproteinases and their inhibitors as well as collagen-IV to attenuate pulmonary fibrosis in rats. *Genet Mol Res*. 2016 Jun 3;15(2). doi: [10.4238/gmr.15027530](https://doi.org/10.4238/gmr.15027530)
- [127] Wang Y, Wang Y, You F, et al. Novel use for old drugs: the emerging role of artemisinin and its derivatives in fibrosis. *Pharmacol Res*. 2020 Jul;157:104829.
- [128] Dolivo D, Weathers P, Dominko T. Artemisinin and artemisinin derivatives as anti-fibrotic therapeutics. *Acta Pharm Sin B*. 2021 Feb;11(2):322–339. doi: [10.1016/j.apsb.2020.09.001](https://doi.org/10.1016/j.apsb.2020.09.001)